The Yin and Yang of How N-terminal Acyl Caps Affect Collagen Triple Helices

Tomas Fiala, Rahel Heeb, Luca Vigliotti, and Helma Wennemers*

Laboratory of Organic Chemistry, ETH Zurich, D-CHAB, Vladimir-Prelog-Weg 3, 8093 Zürich, Switzerland.

KEYWORDS: collagen model peptides • N-terminal acylation • proline • self-assembly

ABSTRACT: N-terminal acylation is a common tool for the installation of functional moieties (e.g., sensors or bioactive molecules) on collagen model peptides (CMPs). The N-acyl group and its length are generally assumed to have little or no influence on the properties of the collagen triple helix formed by the CMP. Here, we show that the length of short (C_1–C_4) acyl capping groups has different effects on the thermal stability of collagen triple helices in POG, OGP, and GPO frames. While the effect of different capping groups on the stability of triple helices in the GPO frame is negligible, longer acyl chains stabilize OGP triple helices but destabilize POG analogs. The observed trends arise from a combination of steric repulsion, the hydrophobic effect, and n → π* interactions. Our study provides a basis for the design of N-terminally functionalized CMPs with predictable effects on triple helix stability.

INTRODUCTION

Collagen is the most abundant protein in mammals and plays a key role in the structural integrity of connective tissues, including skin, cartilage, tendons, ligaments, and bones.[1-3] The structural properties of collagen rely on the formation of triple helices from single strands that adopt polyproline type II (PPII)-helices with all-*trans* amide bonds (Figure 1).[1] A repetitive sequence of three amino acids, Xaa–Yaa–Gly, is characteristic of collagen. Glycine (Gly, G) is required in every third position for tight packing of the triple helix. The amino acids in the Xaa and Yaa positions are variable, but are most commonly (~30%) occupied by proline (Pro, P) and (2*S*,4*R*)-hydroxyproline (Hyp, O), respectively (Figure 1).[4] The triple helix is stabilized by intrastrand n → π* interactions between adjacent amide groups and interstrand H-bonds between the Gly N–H and the Xaa C=O groups (Figure 1).[1,5-7]

Extensive post-translational modifications and cross-linking make it virtually impossible to isolate natural collagen in a pure, homogenous form.[1] Short collagen model peptides (CMPs) are, therefore, useful surrogates of the native protein to study the structural features of the collagen triple helix[1,3,8] and construct supramolecular materials beyond what is known for natural collagen.[9,10]

N-terminal acetyl groups are commonly used as caps to stabilize the triple helical assemblies and make their stability pH-independent.[11,12] Fields showed that long (> C_6) acyl chains stabilize collagen triple helices compared to uncapped N-termini.[13] We have recently unraveled that frame-shifted CMPs ($[POG]_x$, $[OGP]_x$, $[GPO]_x$) form triple helices with significantly different thermal stabilities.[12,14,15] Furthermore, we showed that the stabilizing effect of N-terminal acetylation depends on the frame.[12] These findings prompted us to interrogate whether the length of N-terminal acyl groups affects collagen triple helix stability and whether the effects depend on the CMP frame.

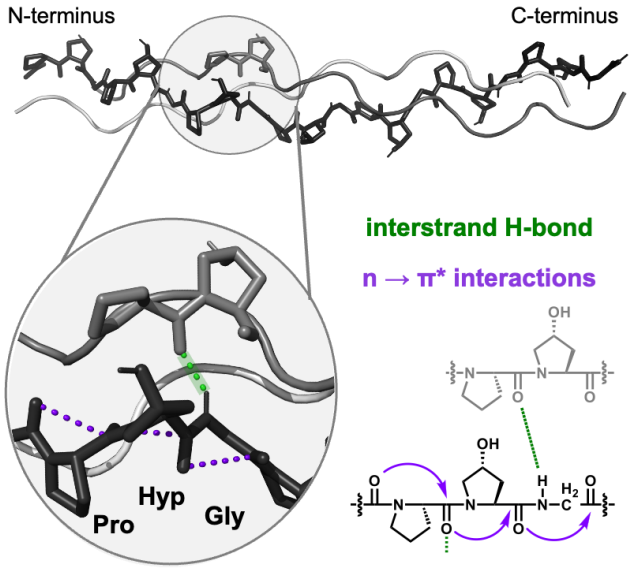

Figure 1. General structure of the collagen triple helix with stabilizing interstrand H-bonds (green) and n → π* interactions (purple).

Herein, we show that the influence of short N-terminal acyl capping groups (C_1–C_4) on collagen triple helix stability depends on the frame. We elucidate that the effects arise from the different relative positions of the acyl moieties depending on whether they are attached at N-terminal Xaa, Yaa, or Gly residues. The results provide a guide for the design of N-terminally functionalized CMPs.

MATERIALS AND METHODS

Materials and reagents were purchased from ABCR, Bachem, Fluorochem, Senn, or Sigma Aldrich at the highest available purity and used without further purification. Water used for peptide preparation and purification was Milli-Q water with a resistivity of 18.2 MΩ.cm, prepared by a Sartorius Arium611VF water purification system (Sartorius, Göttingen, Germany).

Solid phase peptide synthesis was performed using the Fmoc/*t*Bu strategy with a Rink amide ChemMatrix resin (Biotage, Uppsala, Sweden; loading 0.42 mmol/g, 100–200 mesh) on a 100 µmol scale according to the general protocols detailed in the Supporting Information.

High-resolution mass spectrometry (MS) was performed by the Molecular and Biomolecular Analysis (MoBiAs) service of the D-CHAB at ETH Zürich, using a Bruker Daltonics maXis (Bruker Corporation, Billerica, MA, USA) equipped with an ESI (electrospray ionization) source and a Q-TOF ion analyzer.

Circular dichroism (CD) spectroscopic analyses were carried out with a Chirascan Plus (Applied Biophysics Ltd, Leatherhead, UK) using quartz cuvettes with a path length of 1.0 mm (Hellma, 110-QS). The lyophilized CMPs were dissolved in 1× PBS (gibco, 10010-015) at a concentration of 200 µM. The solutions were subsequently annealed by heating to 80 °C for 15 min in a water bath, cooling to room temperature outside of the water bath, and storage at 4 °C for at least 16 h prior to CD spectroscopic analysis and thermal denaturation.

CD Spectra. CD spectra were recorded using a spectral bandwidth of 1 nm at 7 °C with a time constant of 5 s and a step resolution of 1 nm from 190 nm to 260 nm. The data were analyzed using GraphPad PRISM 9 (GraphPad Software, Inc., San Diego, CA, USA).

Thermal denaturation studies. The unfolding of the triple helices was followed at 225 nm with a spectral bandwidth of 1 nm and a time constant of 5 s (2×5 s measurement + 2×2 s shutter delay = 14 s per data point). The temperature was increased in steps of 1 °C from 7 °C to 70 °C and each data point was recorded after an equilibration time of 100 s (overall heating rate = 1 °C/114 s). The recorded data were fitted to an all or none transition in which three single strands combine to a triple helix as previously reported by Engel *et al.* (see Supporting Information for the model).[16,17] The fitting was performed using GraphPad Prism 9 with T_m = 40 °C as an initial value. The T_m values were reproducible with a standard deviation (SD) in the range of ± 0.1 °C to ± 0.4 °C.

Preparative reverse-phase HPLC was performed on a Waters HPLC consisting of a Waters 2555 Quaternary Gradient Module, a Waters 2489 UV/Vis Detector, and a Waters 2767 Sample Manager (Waters Corporation, Milford, MA, USA), equipped with a ReproSil Gold C18 column (250 × 10 mm, 10 µm particle size, 120 Å pore size). Milli-Q water containing 1% acetonitrile and 0.1% TFA (solvent A) and acetonitrile (solvent B) were used as eluents at a flow rate of 20 mL/min and an oven temperature of 50 °C (unless stated otherwise). After purification, all collected fractions were analyzed by analytical HPLC or LC-MS and only pure fractions (> 95%) were combined.

Analytical reverse-phase HPLC was performed using a Dionex UHPLC, Ultimate 3000 from Thermo Fisher Scientific (Waltham, MA, USA) equipped with a Jupiter C18 column (250 × 4.6 mm, 5 µm particle size, 300 Å pore size) from Phenomenex (Danaher, Washington, D.C., USA). Acetonitrile (solvent A) and water containing 1% acetonitrile and 0.1% CF_3CO_2H (solvent B) were used as eluents at a flow rate of 1 mL/min and an oven temperature of 65 °C.

Medium pressure liquid chromatography (MPLC) was performed using a Teledyne Isco CombiFlash System (Teledyne Technologies, Thousand Oaks, CA, USA). The separation was monitored by a UV/Vis detector and an evaporative light scattering detector (ELSD). Separation was performed on RediSep Bronze silica gel columns from Teledyne.

NMR spectra were recorded on a Bruker AV III 600 (600 MHz for ^{1}H, 150 MHz for ^{13}C) at 294 K at a concentration of 80 mM and analyzed with MestReNova (v.14.1.0; Mestrelab Research, S.L., Santiago de Compostela, Spain). Chemical shifts (δ) are reported in parts per million relative to the signal of residual solvent.

$K_{trans/cis}$ equilibrium constants were determined as the ratios between the integral intensities of the formyl group or the ester methyl group signals of the two conformers. The ^{1}H and ^{13}C NMR peaks were unequivocally assigned following the procedures depicted in workflow diagrams in the Supporting Information.

Size-Exclusion Chromatography (SEC) was performed using a Dionex UHPLC, Ultimate 3000 from Thermo Fisher Scientific (Waltham, MA, USA) equipped with a Superdex 30 Increase 10/300 GL column from Cytiva (Danaher, Washington, D.C., USA). 200 mM ammonium acetate buffer (pH 5.0) was used as the eluent at a flow rate of 0.5 mL/min at room temperature. The separation was monitored by a UV detector at 225 nm. 300 µL of the sample used for CD measurements was injected for the analysis.

RESULTS AND DISCUSSION

Thermal stability of collagen triple helices with different acyl capping groups. We started by preparing a series of twelve capped 21-mer CMPs with different N-terminal capping groups and frames (cap–$[POG]_7$–NH_2, cap–$[OGP]_7$–NH_2, cap–$[GPO]_7$–NH_2; Figure 2, Table 1). As N-terminal capping groups, we used formyl (HCO, Fm; C_1), acetyl (CH_3CO, Ac; C_2), propionyl (CH_3CH_2CO, Pr; C_3), and butyryl ($CH_3CH_2CH_2CO$, Bu; C_4) groups. Circular dichroism (CD) spectra of all CMPs showed the characteristic signature of a PPII helix with a local maximum at 225 nm and a minimum close to 200 nm (Figure 3a, Figure S1). Thermal denaturation with CD monitoring at 225 nm provided for all samples sigmoidal curves typical for the cooperative disassembly of the collagen triple helix (Figure 3b, Figure S2). The midpoint of the sigmoidal transition – the melting temperature, T_m – is a characteristic parameter reflecting the relative thermal stability of triple helices.[1]

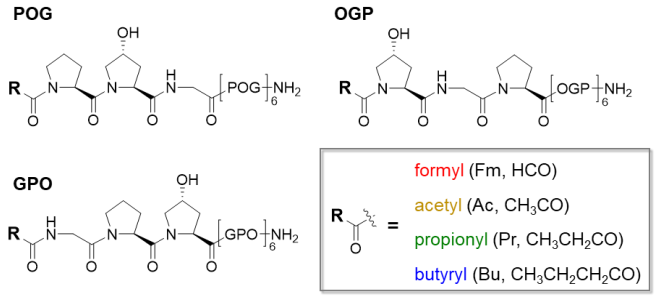

Figure 2. Frame-shifted CMPs with N-terminal capping groups of varying lengths (C_1–C_4).

Table 1. Melting temperatures (T_m) of triple helices with N-terminal acyl groups of varying lengths.[a]

Peptide	N-terminal capping group			
	Formyl (Fm)	Acetyl (Ac)	Propionyl (Pr)	Butyryl (Bu)
cap-[POG]$_7$-NH$_2$	41.0	42.8	41.0	39.6
cap-[OGP]$_7$-NH$_2$	42.7	42.6	44.0	44.7
cap-[GPO]$_7$-NH$_2$	52.9	53.3	53.1	53.5
cap-[GPO]$_6$-NH$_2$	39.2	39.7	39.6	39.9

[a]Melting temperature (T_m) in °C determined by thermal denaturation of a 200 µM peptide solution in phosphate buffered saline (PBS) pH 7.4 with CD monitoring at 225 nm. Heating rate 1 °C/114 s. N = 2-4, standard deviation (SD) < 0.4 °C.

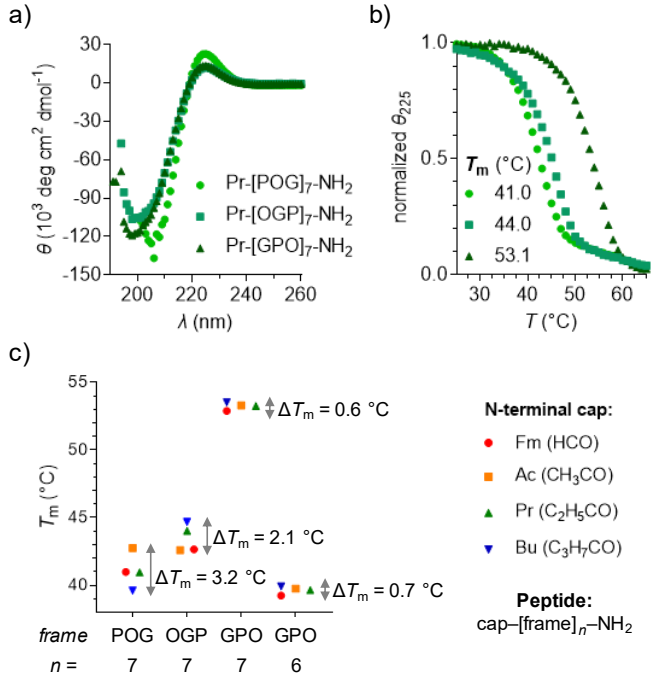

Figure 3. (a) CD spectra and (b) thermal denaturation of triple helices (example of propionyl capped CMPs, see also Figures S1 and S2). (c) Overview of T_m values grouped by frame. Highlighted are T_m distributions within each frame.

The T_m values of the triple helices formed by the CMPs span a range of more than 10 °C and depend, as expected, on the frame. Consistent with our previous studies,[14] the GPO trimers are more stable than the OGP and POG isomers (Table 1, Figure 3c). Size-exclusion chromatography (SEC) confirmed that the CMPs, including those with Bu capping groups, do not form higher-order assemblies beyond the triple helix at a concentration of 200 µM (Figure S3).[11,18]

Effect of different acyl caps depending on the frame. Triple helices with a GPO frame have essentially the same stability (ΔT_m = 0.6 °C), regardless of the length of the N-acyl group (Figure 3c). The differences are higher within the OGP and POG series, with ΔT_m = 2.1 °C and ΔT_m = 3.2 °C, respectively; Figure 3c). We wondered whether the smaller influence of the N-terminal capping group on the stability of [GPO]$_7$ triple helices is related to the GPO frame or caused by the higher overall stability of the cap–[GPO]$_7$–NH$_2$ core compared to the isomers with POG and OGP frames. Hence, we synthesized an analogous series of shorter 18-mer homologs, cap–[GPO]$_6$–NH$_2$, that form triple helices with stabilities comparable to those of the 21-mers with POG and OGP frames. The T_m values within this shorter cap–[GPO]$_6$–NH$_2$ series differ by 0.7 °C, a ΔT_m value similar to that of the cap–[GPO]$_7$–NH$_2$ series and significantly smaller than those of the cap–[POG]$_7$–NH$_2$ and cap–[OGP]$_7$–NH$_2$ series (Table 1, Figure 3c). These results show that N-terminal capping groups affect the stability of triple helices formed by CMPs in the GPO frame the least and those formed by POG-triple helices the most.

Next, we analyzed the stability trends of the capped triple helices within each frame. Within the POG frame, the T_m rises by almost 2 °C from the formyl to the acetyl derivatives but decreases by more than 3 °C upon acyl chain length elongation to butyryl (Figure 4a). In contrast, within the OGP-frame series, the stability of the formyl and acetyl capped triple helices is the same and increases with elongation of the N-acyl cap to butyryl by 2 °C (Figure 4b). The T_m of the triple helices with a GPO frame slowly rises from the formylated to the butyryl analog but the overall increase is small, within or at the edge of the experimental error (Figure 4c).

The nearly opposite stability trends of collagen triple helices with POG and OGP frames with increasing chain lengths of the cap are intriguing. The trimers formed by acetyl capped CMPs Ac–[POG]$_7$–NH$_2$ and Ac–[OGP]$_7$–NH$_2$ have the same stability (T_m = 42.8 and 42.6 °C, respectively; orange in Figure 4d), while the butyryl-capped CMPs Bu–[POG]$_7$–NH$_2$ and Bu–[OGP]$_7$–NH$_2$ have a stability difference of ΔT_m = 5.1 °C (T_m = 39.6 and 44.7 °C, respectively; blue in Figure 4d). What is the reason for these diverse trends?

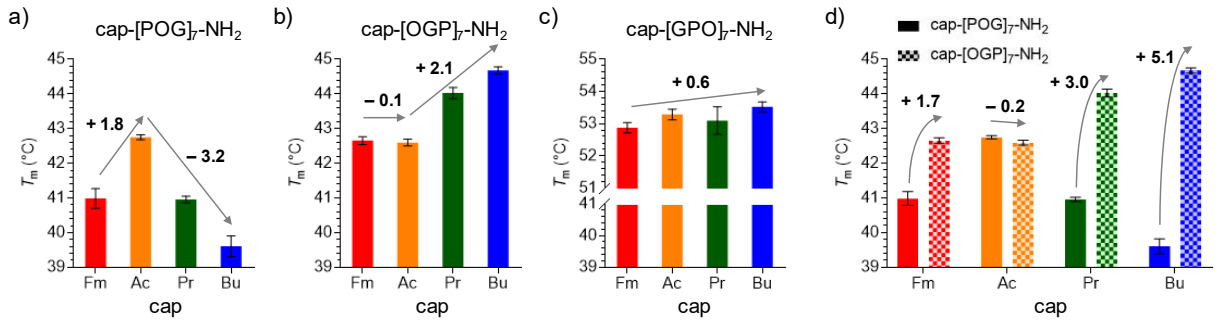

Figure 4. (a-c) Dependence of melting temperatures of collagen triple helices on the N-terminal acyl cap within each collagen frame: (a) POG, (b) OGP, and (c) GPO. (d) Comparison of the melting temperatures of triple helices with POG and OGP frames for each N-terminal acyl cap. Grey arrows highlight the trends; the associated numbers denote the melting temperature differences (ΔT_m) in °C. Error bars represent ± SD.

We hypothesized that three factors could contribute to the observed effects: (1) the *trans*/*cis* equilibrium of the cap amide bond; (2) steric repulsion between the N-terminal capping groups; and (3) stabilization of H-bonds and n → π* interactions by a hydrophobic environment created by the capping groups.

Influence of acyl groups with different chain lengths on the *trans*/*cis* amide bond ratio. Stabilizing intrastrand n → π* interactions and interstrand H-bonds in collagen are only possible with *trans* amide bonds (Figure 5a).[7] Amide bonds of N-terminally capped Gly residues (cap–Gly) are secondary and, thus, almost exclusively *trans*. This consideration is in line with the consistent thermal stability of collagen triple helices with N-terminal Gly residues. In contrast, the amide bonds of capped Pro and Hyp residues are tertiary and also populate the *cis* conformer.[7] To evaluate the effect of different acyl caps on the *trans*/*cis* equilibrium of cap–Pro and cap–Hyp amide bonds, we analyzed eight proline methyl ester derivatives with short *N*-acyl substituents as proxies of the N-terminus of the CMPs (Figure 5b, Table S1). ^{1}H NMR spectra in D_2O revealed that the Hyp derivatives have a higher $K_{trans/cis}$ value compared to the respective Pro derivatives with the same *N*-acyl group. This finding is consistent with a Hyp ψ dihedral angle close to 150°, which is ideal for an n → π* interaction.[7,19] The $K_{trans/cis}$ is lowest in the case of the formylated derivatives Fm-Pro-OMe and Fm-Hyp-OMe (1.8 and 2.7, respectively) and increases with longer acyl substituents; up to $K_{trans/cis}$ = 6.1 and 9.1 for the butyryl derivatives Bu-Pro-OMe and Bu-Hyp-OMe, respectively (Figure 5b).

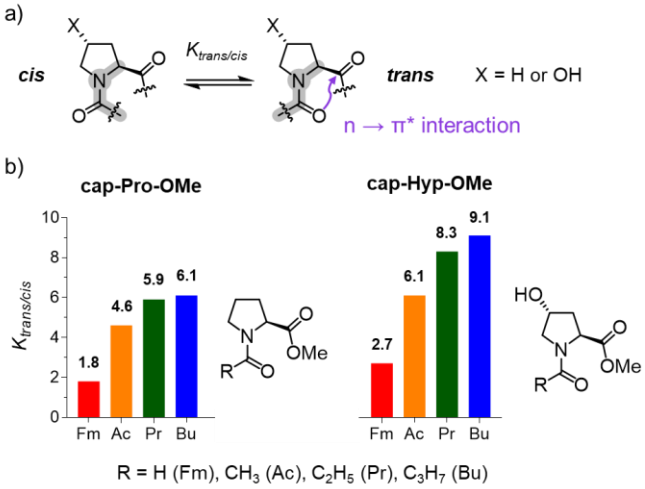

Figure 5. (a) *trans*/*cis* Isomerization of Pro or Hyp amide bonds (grey). The n → π* interaction (purple) is only possible in the *trans* conformation. (b) $K_{trans/cis}$ values of proline derivatives with short *N*-acyl groups determined by ^{1}H NMR spectroscopy of 80 mM solutions in D_2O at 294 K. *Note:* the value of Fm-Pro-OMe is from ref. [20], of Ac-Pro-OMe from ref. [21] and of Ac-Hyp-OMe from ref. [7].

n → π* Interactions between neighboring amides involve delocalization of the non-bonding electrons of O_{i-1} into the π^* orbital of the C_i=O_i bond.[5] In the POG frame, this interaction enhances the electron density of the C=O of the Pro–Hyp bond, which is involved in the interstrand H-bonding with the neighboring strand (Figure 6a).[12] This strengthening of the H-bond is consistent with the increased T_m of the triple helix formed by Ac–[POG]$_7$–NH_2 compared to Fm–[POG]$_7$–NH_2 (Table 1, Figure 4a). The stronger electron donating effect of the methyl group in the Ac cap compared to the hydrogen in the Fm cap could also contribute to this difference. Yet, despite increasing *trans*/*cis* ratios in the Ac < Pr < Bu row of acyl–Pro–OMe derivatives, the thermal stability of the collagen triple helices decreases. This finding indicates that the *trans*/*cis* equilibrium and the ensuing n → π* interaction is not the only factor responsible for the effects of different acyl groups on the thermal stability of collagen triple helices with a POG frame.

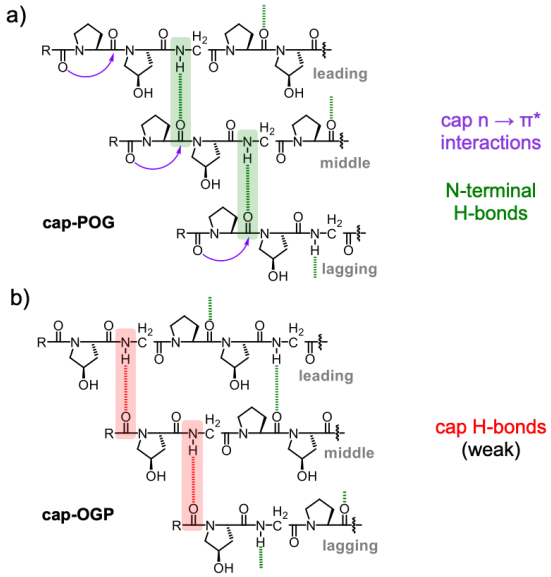

Figure 6. Illustration of the N-terminal regions of (a) cap–$[POG]_n$ and (b) cap–$[OGP]_n$ triple helices. R = H or alkyl.

In the OGP frame, the carbonyl group of the N-terminal *trans* cap–Hyp amide is directly involved in interstrand H-bonding (Figure 6b). Thus, high $K_{trans/cis}$ values of cap–Hyp favor the triple helix, consistent with the observed trend (Figure 4b). Yet, previous molecular dynamics studies suggest that the H-bonds at the N-terminus of triple helices in the OGP frame are weak and lost early in the melting process.[12,14] This insight is in agreement with the similar thermal stability of the triple helices formed by Fm–$[OGP]_7$–NH_2 and Ac–$[OGP]_7$–NH_2 (T_m = 42.7 and 42.6 °C, respectively, despite the higher $K_{trans/cis}$ of the Ac versus Fm methyl ester of Hyp (Table 1, Figure 3b and 5b). Thus, similarly to the POG frame, the *trans/cis* equilibrium of the cap–Hyp amide bond alone does not explain the stability trend of cap–$[OGP]_7$–NH_2 triple helices with increasing cap length.

Influence of steric constraints and the hydrophobic effect. The environment within the repetitive Xaa–Yaa–Gly sequence in collagen triple helices is not identical for the three positions due to the one-residue-stagger with which the three strands wrap around each other.[1] Gly, the smallest amino acid, is tightly packed in the center of the triple helix, while the side chains of the amino acids in Xaa (Pro) and Yaa (Hyp) positions point outwards.[22] The capping groups are, in essence, surrogates of the amino acid that precedes the N-terminal residue: Gly for the POG frame, Pro for the OGP frame, and Hyp for the GPO frame (Figure 7). We reasoned that the different steric environments of Gly, Xaa, and Yaa, and thus, the capping groups, affect triple helix stability. We, therefore, used a crystal structure of collagen (PDB ID 3B0S)[23] to build models of collagen triple helices with the three frames carrying N-terminal butyryl caps. In the model of the Bu–$[POG]_7$–NH_2 derived triple helix, the capping groups point towards the middle of the triple helix, whereas they point to the outside in the OGP and GPO isomers (Figure 7).

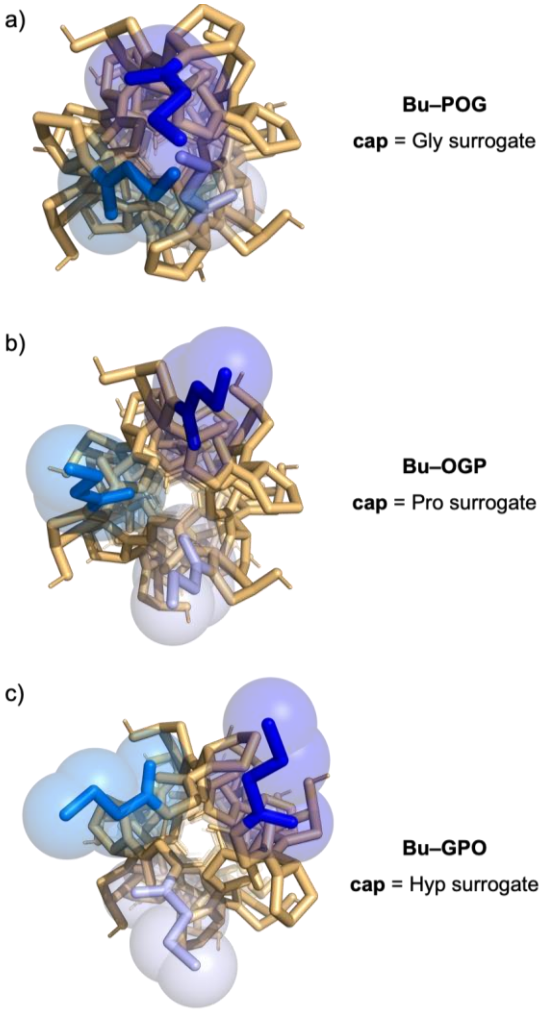

Figure 7. Top view (from the N-terminal side) of a $[POG]_7$ (a), $[OGP]_7$ (b), and $[GPO]_7$ (c) triple helix model bearing an N-terminal butyryl cap (derived from a CMP crystal structure, PDB ID 3B0S).[23] Color code: amino acid residues (beige), butyryl caps (blue). For simplicity, the models were built with the butyryl groups in an all-anti conformation.

The model of the POG frame illustrates that the acetyl group is the largest N-terminal cap that can be accommodated without steric constraints (Figure 7a and S3a). Unlike an N-terminal Gly residue, which forms H-bonds to the adjacent strand, propionyl, butyryl, and longer N-terminal acyl tails cannot compensate for the steric constraints (Figure S4b,c). This steric clash between large capping groups attached to an N-terminal Pro is reminiscent of collagen triple helix destabilization by mutation of Gly into a sterically more demanding amino acid that causes the brittle bone disease (*osteogenesis imperfecta*).[24] The steric constraints overwrite the stabilizing effect of the favorable *trans*/*cis* ratio and ensuing n → π* interaction and thus explain the significantly lower triple helix stability of Pr–$[POG]_7$–NH_2 (T_m = 41.0 °C) and Bu–$[POG]_7$–NH_2 (T_m = 39.6 °C) compared to Ac–$[POG]_7$–NH_2 (T_m = 42.8 °C; Table 1, Figure 4a).

Within the OGP and GPO frames, the models corroborate the expected outward orientation of the capping groups without steric constraints (Figure 7b,c). The alkyl chains of

the caps create a hydrophobic patch at the N-terminus. Such local hydrophobic environments strengthen H-bonding, enhance the *trans*/*cis* ratio of amide bonds, and, thus, $n \rightarrow \pi^*$ interactions.[21] This analysis is consistent with previous studies on lipidated triple helices[25,26] and explains the stabilizing effect with increasing alkyl chain lengths (ΔT_m = 2.1 °C for OGP and ΔT_m = 0.6 °C for GPO; Figure 4b,c). The stabilization is more prominent for the OGP frame since (i) the local hydrophobic environment affects the *trans*/*cis* equilibrium of the tertiary cap–Hyp amide bond more than the secondary cap–Gly amide; and (ii) Hyp is the least favored N-terminal amino acid for capped collagen triple helices,[14] which benefits the most from hydrophobic stabilization.

CONCLUSIONS

In summary, short (C_1–C_4) N-terminal acyl capping groups have different effects on the thermal stability of collagen triple helices depending on their frame. Capping groups influence the stability of trimers with the GPO frame only negligibly but affect triple helices with POG and OGP frames to significant extents. The effect of the length of the N-terminal cap is opposite in POG and OGP frames: triple helices formed by Ac–$[POG]_7$–NH_2 and Ac–$[OGP]_7$–NH_2 have almost identical melting temperatures, but the butyryl analogs Bu–$[POG]_7$–NH_2 and Bu–$[OGP]_7$–NH_2 melt more than 5 °C apart. Structural analysis of the frame-shifted CMPs and model compounds revealed that the effects arise from a combination of steric constraints, the *trans*/*cis* isomerization of cap amide bonds, and the enhancement of H-bonding through $n \rightarrow \pi^*$ interactions and the hydrophobic effect.

N-terminal acyl groups are commonly used as extensions of CMPs to introduce functional moieties. These include, e.g., sensors or cargo of collagen hybridizing peptides,[27-30] or oligomerizing functionalities for the construction of collagen-based materials.[10,31-34] Our findings provide a basis for the rational selection of the collagen frame together with the acyl extension depending on the requirements for triple helix stability and directionality of the N-terminal group.

ASSOCIATED CONTENT

This material is available free of charge via the Internet at http://pubs.acs.org. Figures referenced in the main text, Synthesis and analytical data of CMPs, Thermal denaturation model, Synthesis and analytical data of proline derivatives, $K_{trans/cis}$ determination by NMR spectroscopy.

AUTHOR INFORMATION

Corresponding Author

***Helma Wennemers** – Laboratory of Organic Chemistry, ETH Zurich, D-CHAB, Vladimir-Prelog-Weg 3, 8093 Zurich, Switzerland;
http://orcid.org/0000-0002-3075-5741;
Email: helma.wennemers@org.chem.ethz.ch

Authors

Tomas Fiala - Laboratory of Organic Chemistry, ETH Zurich, D-CHAB, Vladimir-Prelog-Weg 3, 8093 Zurich, Switzerland;
https://orcid.org/0000-0001-6949-4561;

Rahel Heeb - Laboratory of Organic Chemistry, ETH Zurich, D-CHAB, Vladimir-Prelog-Weg 3, 8093 Zurich, Switzerland;
https://orcid.org/0000-0003-2592-7040;

Luca Vigliotti - Laboratory of Organic Chemistry, ETH Zurich, D-CHAB, Vladimir-Prelog-Weg 3, 8093 Zurich, Switzerland;

Author Contributions

T.F. and H.W. conceptualized the project. R.H. and T.F. synthesized the peptides and carried out the CD-spectroscopic experiments. L.V., R.H. and T.F. synthesized the model proline derivatives and determined the *trans*/*cis* ratios. H.W. oversaw the project. T.F. and H.W. wrote the manuscript. All authors edited the manuscript and approved its final version.

Notes

The authors declare no competing financial interests.

ACKNOWLEDGMENT

We thank the Swiss National Science Foundation (SNF grant 200020_207505) for financial support. This project has received funding from the European Union's Horizon 2020 research and innovation program under the Marie Sklodowska-Curie grant agreement No. 891009 (T.F.). We thank Philipp Bittner for help with SEC experiments, the NMR Service of the Laboratory of Organic Chemistry for NMR measurements, and the Molecular and Biomolecular Analysis Service (MoBiAS) for HRMS measurements.

REFERENCES

(1) Shoulders, M. D.; Raines, R. T. Collagen Structure and Stability. *Annu. Rev. Biochem.* **2009**, *78* (1), 929-958. DOI: 10.1146/annurev.biochem.77.032207.120833.

(2) Bella, J. Collagen structure: new tricks from a very old dog. *Biochem. J.* **2016**, *473* (8), 1001-1025. DOI: 10.1042/bj20151169.

(3) Hulgan, S. A. H.; Hartgerink, J. D. Recent Advances in Collagen Mimetic Peptide Structure and Design. *Biomacromolecules* **2022**, *23* (4), 1475-1489. DOI: 10.1021/acs.biomac.2c00028.

(4) Ramshaw, J. A. M.; Shah, N. K.; Brodsky, B. Gly-X-Y Tripeptide Frequencies in Collagen: A Context for Host–Guest Triple-Helical Peptides. *J. Struct. Biol.* **1998**, *122* (1), 86-91. DOI: 10.1006/jsbi.1998.3977.

(5) Newberry, R. W.; Raines, R. T. The n→π* Interaction. *Acc. Chem. Res.* **2017**, *50* (8), 1838-1846. DOI: 10.1021/acs.accounts.7b00121.

(6) Wilhelm, P.; Lewandowski, B.; Trapp, N.; Wennemers, H. A Crystal Structure of an Oligoproline PPII-Helix, at Last. *J. Am. Chem. Soc.* **2014**, *136* (45), 15829-15832. DOI: 10.1021/ja507405j.

(7) Bretscher, L. E.; Jenkins, C. L.; Taylor, K. M.; DeRider, M. L.; Raines, R. T. Conformational Stability of Collagen Relies on a Stereoelectronic Effect. *J. Am. Chem. Soc.* **2001**, *123* (4), 777-778. DOI: 10.1021/ja005542v.

(8) Engel, J.; Bächinger, H. P. Structure, Stability and Folding of the Collagen Triple Helix. In *Topics in Current Chemistry*, Springer Berlin Heidelberg, 2005; pp 7-33.

(9) Fields, G. B. Synthesis and biological applications of collagen-model triple-helical peptides. *Org. Biomol. Chem.* **2010**, *8* (6), 1237. DOI: 10.1039/b920670a.

(10) Strauss, K.; Chmielewski, J. Advances in the design and higher-order assembly of collagen mimetic peptides for regenerative medicine. *Curr. Opin. Biotechnol.* **2017**, *46*, 34-41. DOI: 10.1016/j.copbio.2016.10.013.

(11) Egli, J.; Erdmann, R. S.; Schmidt, P. J.; Wennemers, H. Effect of N- and C-terminal functional groups on the stability of collagen triple helices. *Chem. Commun.* **2017**, *53* (80), 11036-11039. DOI: 10.1039/c7cc05837c.

(12) Fiala, T.; Barros, E. P.; Heeb, R.; Riniker, S.; Wennemers, H. Predicting Collagen Triple Helix Stability through Additive Effects of Terminal Residues and Caps. *Angew. Chem., Int. Ed.* **2023**, *62* (3), e202214728. DOI: 10.1002/anie.202214728.

(13) Yu, Y.-C.; Tirrell, M.; Fields, G. B. Minimal Lipidation Stabilizes Protein-Like Molecular Architecture. *J. Am. Chem. Soc.* **1998**, *120* (39), 9979-9987. DOI: 10.1021/ja981654z.

(14) Fiala, T.; Barros, E. P.; Ebert, M.-O.; Ruijsenaars, E.; Riniker, S.; Wennemers, H. Frame Shifts Affect the Stability of Collagen Triple Helices. *J. Am. Chem. Soc.* **2022**, *144* (40), 18642-18649. DOI: 10.1021/jacs.2c08727.

(15) Qi, Y.; Zhou, D.; Kessler, J. L.; Qiu, R.; Yu, S. M.; Li, G.; Qin, Z.; Li, Y. Terminal repeats impact collagen triple-helix stability through hydrogen bonding. *Chem. Sci.* **2022**, *13* (42), 12567-12576. DOI: 10.1039/d2sc03666e.

(16) Engel, J.; Chen, H.-T.; Prockop, D. J.; Klump, H. The triple helix – coil conversion of collagen-like polytripeptides in aqueous and nonaqueous solvents. Comparison of the thermodynamic parameters and the binding of water to $(L\text{-Pro-L-Pro-Gly})_n$ and $(L\text{-Pro-L-Hyp-Gly})_n$. *Biopolymers* **1977**, *16* (3), 601-622. DOI: 10.1002/bip.1977.360160310.

(17) Frank, S.; Kammerer, R. A.; Mechling, D.; Schulthess, T.; Landwehr, R.; Bann, J.; Guo, Y.; Lustig, A.; Bächinger, H. P.; Engel, J. Stabilization of short collagen-like triple helices by protein engineering. *J. Mol. Biol.* **2001**, *308* (5), 1081-1089. DOI: 10.1006/jmbi.2001.4644.

(18) Kar, K.; Amin, P.; Bryan, M. A.; Persikov, A. V.; Mohs, A.; Wang, Y.-H.; Brodsky, B. Self-association of Collagen Triple Helic Peptides into Higher Order Structures. *J. Biol. Chem.* **2006**, *281* (44), 33283-33290. DOI: 10.1074/jbc.m605747200.

(19) Berisio, R.; Vitagliano, L.; Mazzarella, L.; Zagari, A. Crystal structure of the collagen triple helix model $[(\text{Pro-Pro-Gly})_{10}]_3$. *Protein Sci.* **2002**, *11* (2), 262-270. DOI: 10.1110/ps.32602.

(20) Hinderaker, M. P.; Raines, R. T. An electronic effect on protein structure. *Protein Sci.* **2003**, *12* (6), 1188-1194. DOI: 10.1110/ps.0241903.

(21) Siebler, C.; Maryasin, B.; Kuemin, M.; Erdmann, R. S.; Rigling, C.; Grünenfelder, C.; Ochsenfeld, C.; Wennemers, H. Importance of dipole moments and ambient polarity for the conformation of Xaa–Pro moieties – a combined experimental and theoretical study. *Chem. Sci.* **2015**, *6* (12), 6725-6730. DOI: 10.1039/c5sc02211h.

(22) Persikov, A. V.; Ramshaw, J. A. M.; Brodsky, B. Collagen model peptides: Sequence dependence of triple-helix stability. *Biopolymers* **2000**, *55* (6), 436-450. DOI: https://doi.org/10.1002/1097-0282(2000)55:6<436::AID-BIP1019>3.0.CO;2-D.

(23) Okuyama, K.; Miyama, K.; Mizuno, K.; Bächinger, H. P. Crystal structure of $(\text{Gly-Pro-Hyp})_9$: Implications for the collagen molecular model. *Biopolymers* **2012**, *97* (8), 607-616. DOI: 10.1002/bip.22048.

(24) Beck, K.; Chan, V. C.; Shenoy, N.; Kirkpatrick, A.; Ramshaw, J. A. M.; Brodsky, B. Destabilization of osteogenesis imperfecta collagen-like model peptides correlates with the identity of the residue replacing glycine. *Proc. Natl. Acad. Sci.* **2000**, *97* (8), 4273-4278. DOI: 10.1073/pnas.070050097.

(25) Egli, J.; Esposito, C.; Müri, M.; Riniker, S.; Wennemers, H. Influence of Lipidation on the Folding and Stability of Collagen Triple Helices—An Experimental and Theoretical Study. *J. Am. Chem. Soc.* **2021**, *143* (15), 5937-5942. DOI: 10.1021/jacs.1c01512.

(26) Egli, J.; Siebler, C.; Köhler, M.; Zenobi, R.; Wennemers, H. Hydrophobic Moieties Bestow Fast-Folding and Hyperstability on Collagen Triple Helices. *J. Am. Chem. Soc.* **2019**, *141* (14), 5607-5611. DOI: 10.1021/jacs.8b13871.

(27) Chattopadhyay, S.; Raines, R. T. Collagen-based biomaterials for wound healing. *Biopolymers* **2014**, *101* (8), 821-833. DOI: 10.1002/bip.22486.

(28) Dones, J. M.; Tanrikulu, I. C.; Chacko, J. V.; Schroeder, A. B.; Hoang, T. T.; Gibson, A. L. F.; Eliceiri, K. W.; Raines, R. T. Optimization of interstrand interactions enables burn detection with a collagen-mimetic peptide. *Org. Biomol. Chem.* **2019**, *17* (46), 9906-9912. DOI: 10.1039/c9ob01839e.

(29) Aronoff, M. R.; Hiebert, P.; Hentzen, N. B.; Werner, S.; Wennemers, H. Imaging and targeting LOX-mediated tissue remodeling with a reactive collagen peptide. *Nat. Chem. Biol.* **2021**, *17* (8), 865-871. DOI: 10.1038/s41589-021-00830-6.

(30) Wahyudi, H.; Reynolds, A. A.; Li, Y.; Owen, S. C.; Yu, S. M. Targeting collagen for diagnostic imaging and therapeutic delivery. *J. Controlled Release* **2016**, *240*, 323-331. DOI: 10.1016/j.jconrel.2016.01.007.

(31) Cejas, M. A.; Kinney, W. A.; Chen, C.; Leo, G. C.; Tounge, B. A.; Vinter, J. G.; Joshi, P. P.; Maryanoff, B. E. Collagen-Related Peptides: Self-Assembly of Short, Single Strands into a Functional Biomaterial of Micrometer Scale. *J. Am. Chem. Soc.* **2007**, *129* (8), 2202-2203. DOI: 10.1021/ja066986f.

(32) Chen, C.-C.; Hsu, W.; Kao, T.-C.; Horng, J.-C. Self-Assembly of Short Collagen-Related Peptides into Fibrils via Cation−π Interactions. *Biochemistry* **2011**, *50* (13), 2381-2383. DOI: 10.1021/bi1018573.

(33) Luo, T.; Kiick, K. L. Noncovalent Modulation of the Inverse Temperature Transition and Self-Assembly of Elastin-*b*-Collagen-like Peptide Bioconjugates. *J. Am. Chem. Soc.* **2015**, *137* (49), 15362-15365. DOI: 10.1021/jacs.5b09941.

(34) Sun, X.; He, M.; Wang, L.; Luo, L.; Wang, J.; Xiao, J. Luminescent Biofunctional Collagen Mimetic Nanofibers. *ACS Omega* **2019**, *4* (15), 16270-16279. DOI: 10.1021/acsomega.9b00740.

FOR TABLE OF CONTENTS USE ONLY

The Yin and Yang of How N-terminal Acyl Caps Affect Collagen Triple Helices

Tomas Fiala, Rahel Heeb, Luca Vigliotti, and Helma Wennemers*